

Reactions of He⁺, Ne⁺, and Ar⁺ with CH₄, C₂H₆, SiH₄, and Si₂H₆

H. Chatham, D. Hils, R. Robertson, and A. C. Gallagher

Citation: *The Journal of Chemical Physics* **79**, 1301 (1983); doi: 10.1063/1.445884

View online: <http://dx.doi.org/10.1063/1.445884>

View Table of Contents: <http://scitation.aip.org/content/aip/journal/jcp/79/3?ver=pdfcov>

Published by the [AIP Publishing](#)

Articles you may be interested in

High temperature reaction kinetics of CN($v = 0$) with C₂H₄ and C₂H₆ and vibrational relaxation of CN($v = 1$) with Ar and He

J. Chem. Phys. **138**, 124308 (2013); 10.1063/1.4795206

Energy distribution of ion species in Ar/CH₄, Ar/C₂H₂, and Ar/C₃H₆ radiofrequency plasmas

AIP Conf. Proc. **799**, 375 (2005); 10.1063/1.2134643

Refractivity virial coefficients of gaseous CH₄, C₂H₄, C₂H₆, CO₂, SF₆, H₂, N₂, He, and Ar

J. Chem. Phys. **94**, 5669 (1991); 10.1063/1.460478

Molecular beam measurements of inelastic cross sections for transitions between defined rotational states (j, m) of CsF in collisions with He, Ne, Ar, Kr, CH₄, CF₄, SF₆, C₂H₆, N₂, CO, CO₂, N₂O, CH₃Cl, CH₃Br, CF₃H, and CF₃Br

J. Chem. Phys. **71**, 1722 (1979); 10.1063/1.438524

Diffusivity of 3He, 4He, H₂, D₂, Ne, CH₄, Ar, Kr, and CF₄ in (C₄F₉)₃N

J. Chem. Phys. **55**, 4715 (1971); 10.1063/1.1675569



Reactions of He⁺, Ne⁺, and Ar⁺ with CH₄, C₂H₆, SiH₄, and Si₂H₆

H. Chatham, D. Hils, R. Robertson, and A. C. Gallagher^{a)}

Joint Institute for Laboratory Astrophysics, University of Colorado and National Bureau of Standards, Boulder, Colorado 80309

(Received 29 March 1983; accepted 29 April 1983)

The rate coefficients and product-ion distributions for the reactions of He⁺ and Ar⁺ with silane and disilane have been measured in a drift tube, typically for collision energies of 0.01–1 eV. The total charge-exchange rate coefficients are found to be roughly independent of E/N , or collision energy, and are about equal to the Langevin values for the reactions of He⁺ with SiH₄ and C₂H₆ and Ar⁺ with CH₄ and C₂H₆. The He⁺ rate coefficients on CH₄ and Si₂H₆, and the Ne⁺ rate coefficients on SiH₄ and Si₂H₆ are 50% to 80% of the Langevin values, while the Ar⁺ rate coefficients on SiH₄ and Si₂H₆ are much smaller. Product ions tend to be hydrogen poor with very infrequent breaking of the C–C or Si–Si bonds. Furthermore, hydrogen stripping is more severe for the silanes than the alkanes. These product-ion distributions bear no resemblance to the product-ion distributions of either photoionization or electron collisional ionization.

I. INTRODUCTION

The rate coefficients and the products of inert gas ion collisions with silane or disilane are pertinent to an understanding of the discharge chemistry and behavior of glow discharges in inert gas–silane mixtures used to produce amorphous silicon thin films. Previous measurements of the rate coefficients for the reactions SiH_n⁺ + SiH₄ at thermal energies and above by Lampe and collaborators¹ provide information on one ion production source term. Here, we study another major production source: the charge-transfer reactions of inert gas ions with silane or disilane. Comparisons of these rate coefficients to equivalent hydrocarbons are also of interest for understanding these dissociative-ionizing reactions, so we have also studied reactions of the inert gas ions with methane and ethane.

Several methods have been established for measuring ion neutral reaction rate coefficients at thermal energies and above, notably the flowing afterglow,² ion cyclotron resonance technique,³ the mass-selected ion flow tube,⁴ and the drift tube technique⁵ used here. A detailed review of these techniques is given by McDaniel *et al.*⁶

Reactions between ions A⁺ and neutral reactant B,



deplete the concentration of reactant ion A⁺ at the end of a drift tube according to

$$[A^+] = [A_0^+] \exp(-[B]kt), \quad (2)$$

where [B] is the reactant density, [A₀⁺] the concentration of A⁺ when [B] = 0, t is the time in the drift tube, and k the reaction rate coefficient. (The drift velocity greatly exceeds the gas flow velocity in our experiment, so that $t = L/v_d$.) The reactant B is a minor constituent in the inert gas A, and the drift velocity v_d of the inert gas ions A⁺ in the parent gas is determined at a given applied electric field to gas density ratio E/N from the

compilation of previously measured values in Ref. 7. (We have checked v_d for Ar⁺ in Ar and obtained agreement within our uncertainty.) From the decrease in the inert gas ion signal due to the addition of the neutral reactant, the total reaction rate coefficient is determined for a given applied electric field to gas density ratio E/N . By varying E/N , the rate coefficient is determined as a function of the ion kinetic energy.

We assume, in presenting our results, that the average center-of-mass collisional kinetic energy $\langle E_{cm} \rangle$ is given by⁸

$$\langle E_{cm} \rangle = M/(m+M)[\langle E_{ion} \rangle - 3/2 kT] + 3/2 kT, \quad (3)$$

where m is the A⁺ mass, M is the mass of the neutral reactant B, and $\langle E_{ion} \rangle$ is given by Wannier's expression,⁹

$$\langle E_{ion} \rangle = 1/2 m v_d^2 + 1/2 M_b v_d^2 + 3/2 kT, \quad (4)$$

where M_b is the mass of the buffer gas A.

II. EXPERIMENT

A. Apparatus

The apparatus is shown in Fig. 1. An ion source located within the drift tube produces ions by electron impact with a magnetically confined (400 G) beam of electrons of approximately 0.5 eV energy width produced by a tungsten filament. The ions are drifted 1.9 cm out of the source by the repeller field (0.5–18 V/cm) through a 1 cm diam aperture into the 21 cm drift region. Primary and secondary ions are sampled by an 0.08 cm aperture at the end of the drift tube and focused by an assembly of six lens elements into the quadrupole mass spectrometer. Mass-selected ions are detected by an electron multiplier. In measuring rate constants, the inert gas ion signal [A₀⁺] is obtained for 0.10 Torr of inert gas present in the tube; then a known density of reactant gas (0–10⁻³ Torr) is introduced and the depleted inert gas ion signal [A⁺] measured.

The inert and reactant gases are mixed before being

^{a)}Staff Member, Quantum Physics Division, National Bureau of Standards.

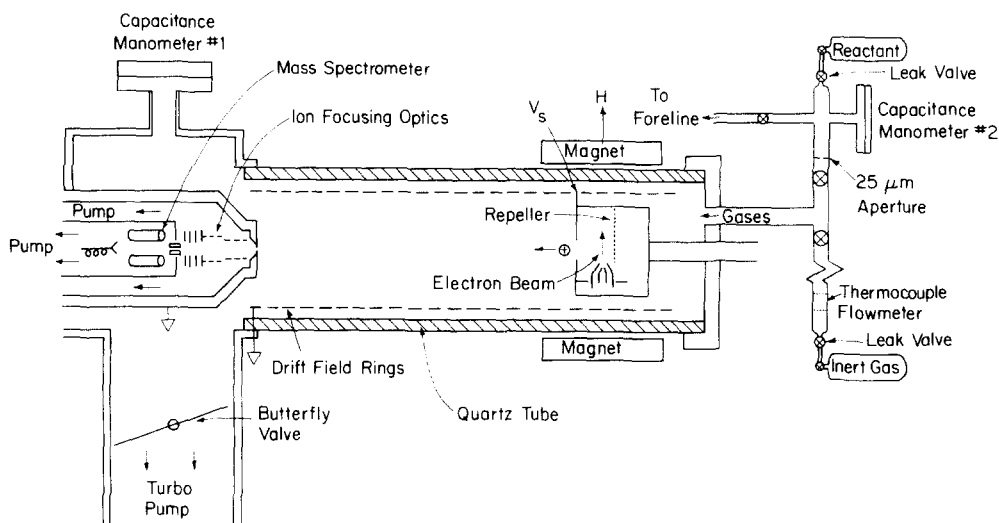


FIG. 1. Apparatus: The source and drift regions, of 21 cm length, are enclosed in a 9 cm i.d. quartz tube, and are drawn to scale. The remaining parts are shown diagrammatically.

admitted to the drift tube chamber through a port at the upstream end of the drift tube. Inert gas flow, typically 0.1 Torr ℓ/s , is measured by a thermocouple flow meter and pressure in the drift-tube region, 0.10 Torr, is measured by a capacitance manometer. For reasons discussed below, the much smaller flows of the reactant gas (typically 10^{-4} Torr ℓ/s) are admitted to the gas line from the reactant gas manifold through a 25 μm diam orifice and a valve past the orifice is used to switch the reactant gas rapidly on and off. Pressures of 0–10 Torr in the manifold are measured with a capacitance manometer, with a typical pressure of 1 Torr producing 5×10^{-5} Torr in the drift tube.

Gas flow is maintained by the turbomolecular pump located at the downstream end of the chamber. A butterfly valve reduces the pumping speed of the pump from 200 to 1.5 ℓ/s , so that the gas flow velocity is negligible compared with the ion drift velocity. (The gas flow velocity is 50 cm/s while the lowest drift velocity is 6×10^3 cm/s for Ar⁺ in Ar at $E/N = 14$ Td.⁷) Also, at these low flows there is a negligible pressure drop along the tube. The temperature of the neutral gas in the drift tube is equal to room temperature 300 K. The focusing and mass spectrometer regions are each differentially pumped by oil diffusion pumps with freon-cooled baffles. After baking the system, background gas pressures of 5×10^9 Torr are measured on ionization gauges in these two regions. Typical background gas pressures in the drift tube are 5×10^{-8} Torr with the butterfly valve open and 7×10^{-7} Torr when the valve is throttled to 1.5 ℓ/s pumping speed. With 0.10 Torr of inert gas in the drift tube, pressures of 5×10^{-5} and 5×10^{-7} Torr are maintained in the focusing and mass spectrometer regions, respectively.

The reactivity of the silane gases with oxygen necessitates the decomposition of these gases before venting them into the atmosphere. Thermal decomposition ovens operating at 900 °C are used on the two roughing lines; between the turbomolecular pump and the rough pump, and between the diffusion pumps and the rough pump to pyrolytically decompose the gases into a silicon film and hydrogen gas.

B. Impurities

Impurity effects are unimportant for the following reasons. Impurities present in the inert gas or in the drift tube will not change when the reactant is introduced and thus will not affect the rate constant measurement. Impurities present in the reactant gases as well as in the chamber and the inert gases are negligible, as seen in the secondary ion spectra (see Ref. 10). Impurity levels from the drift chamber are minimized by using an adequate pumping speed (1.5 ℓ/s). Typical impurity ion-signal levels as a percentage of the inert gas ion signal are roughly 0.2% for N⁺, O⁺, and N₂⁺; 0.3% for OH⁺ and less than 0.3% for H₂O⁺ in He or Ne; 2% for H₂O⁺, Ar²⁺, and ArH⁺ in Ar; 0.5% for Ne²⁺ and less than 0.5% for NeH⁺ in Ne; and less than 0.1% for He²⁺, HeH⁺, He₂⁺, Ne₂⁺, and Ar₂⁺.

C. Ion source

Electron emission currents collected on the ionizer grid (see Fig. 1) are typically in the range 5×10^{-9} – 10^{-7} A for 50 or 100 eV electron energy. The electron current i_e in the source is adjusted so that the inert gas ion signal is linear in the electron current to within a few percent across a decade in i_e . Ion currents produced in the source, measured by applying a 2 V collection potential to the repeller, are in the range 5×10^{-10} – 5×10^{-9} A for the electron currents given above.

All of the reactant gases produce some change, generally reversible, in the electron current when they are added (at less than 0.5% concentration) to the inert gas; the largest effect (+15%) is for silane and disilane. When the electron emission current was adjusted to be constant, the number of ions collected on the repeller was constant for the alkanes but decreased 35% for the silanes. This effect could have caused severe difficulties for the measurements, but the magnitude of the changes decreased upon repeated additions and removals of the reactant and vanished after about 30 min of such treatment. Data were collected after stabilization of the ion and electron currents. These two effects were attributed to carbon and silicon film buildup on surfaces

in the source, primarily due to thermal decomposition on the hot filament.

Electric fields in the source are set in one of two modes. In the usual mode of operation, the grid and repeller potentials are set so that the source field equals the drift field. The time the ions spend in the source ($1.9 \text{ cm}/v_d$) is then added to the time spent in the drift tube ($21 \text{ cm}/v_d$) in computing the rate constant. In the second mode, used to check for space charge effects in the source (discussed below), the source field is set at a constant value 18.6 V/cm that is considerably greater than the drift field. In this mode, the much shorter time t_s the ions spend in the source is added to the drift tube time of $21 \text{ cm}/v_d$; t_s thus varies from 1% to 9% of the total drift time as E/N is varied.

Space charge effects in the source would be a problem if the ion density n is large enough to cause significant modification of the source fields. However, a calculation¹⁰ of the space charge modification of the applied fields in the source chamber shows a 7% change in the field in the vicinity of the electron beam for the lowest source field used (1 V/cm). Since t_s is much less than t , this minor change in t_s has a negligible effect on the results. This was confirmed by measurements of the rate constants using both source modes which agree within 10% at low E/N (for He⁺ + Si₂H₆), whereas with the high source fields in the second mode (18.6 V/cm) would greatly reduce the ion density and any space charge effects. Space charge effects in the drift tube would be a problem if the ion density did not satisfy $n \ll E/4\pi eL$, where L is the relevant length of the apparatus and E is the electric field.¹¹ Thus $n \ll 2.6 \times 10^4$ ions/cm³ is required for the lowest source field and $L = 21 \text{ cm}$. The actual ion densities in the drift chamber can be estimated from measurements of the ion current collected on the drift field rings (appropriately biased) using the approximation, $n = i_{\text{ion}}/\pi a^2 v_d e$. A typical value of i_{ion} collected in the drift tube (for He⁺) is $5 \times 10^{-10} \text{ A}$, giving an ion density of 7×10^2 ions/cm³ in the drift tube (calculated using $v_d = 10^5 \text{ cm/s}$ and $a = 3.8 \text{ cm}$). Thus space charge effects should be negligible in the drift tube. Another indication of negligible space-charge effects is the lack of significant E/N dependence on k at low E/N where $\langle E_{\text{cm}} \rangle$ is nearly constant but the ion density undergoes large changes.

Metastables produced in the source have no effect on the total rate constant measurements and have little effect on the product distribution, as checked by reversing the field of the repeller. For example, the product-ion signals fall to a few percent of their original values when the repeller field is reversed for the reaction He⁺ + CO₂. Metastables are further discussed in Sec. IV D.

D. Reactant density

The pressure of the reactant gas in the drift tube P_r is determined by calibrating the reactant pressure P_m (0.5–10 Torr) in the reactant gas manifold against the pressure P_r (2.5×10^{-5} – 5×10^{-4} Torr) in the drift tube. This was done by first introducing sufficient reactant (10^{-3} Torr) to obtain a reliable capacitance ma-

nometer reading and thereby calibrating the ion signal collected on the repeller against the capacitance manometer at 10^{-3} Torr, then using the repeller as a low current "ion gauge."

The flow rate of the reactant gas through the $25 \mu\text{m}$ orifice is unaffected by the introduction of the inert gas into the drift tube since the mean-free path is much larger than the orifice and in steady state there is no flow of inert gas through the orifice. Thus if the rate of pumping away reactant gas were unaffected by the presence of the inert gas, the above calibration of P_r/P_m in the absence of inert gas would still hold. (At 0.1 Torr and 1.5 l/s pumping speed the reactant gas essentially diffuses throughout the tube, in contrast to the flowing afterglow conditions where it is carried at the buffer gas stream velocity.) We find that P_r/P_m is unaffected by the introduction of the inert gas for reactant and inert gases of comparable masses but not for the heavier reactants in helium or neon. This occurs because the size of the butterfly valve opening is comparable to the mean-free path and the reactant is partially dragged through by the lighter, faster inert gas. However, in the limit of no pumping or zero flow this effect disappears. Thus the rate constants have been measured as a function of butterfly valve limited pumping speed (recalibrating P_r/P_m at each butterfly valve setting) at constant inert gas pressure to obtain the zero-flow limit.¹⁰ This gives corrections to the 1.5 l/s pumping speed data in the range 13%–30% for Ne⁺ and 27%–40% for He⁺, with the largest correction for the heaviest reactant. As just noted, insignificant variation of the Ar⁺ rate constant is seen, as expected due to the similar masses of Ar and reactants. As a secondary ($\pm 15\%$) check on this absence of Ar⁺ correction, we introduced 1.00×10^{-3} Torr of reactant SiH₄ into the drift tube at 1.5 l/s pumping speed, added argon until the capacitance manometer read $0.10100 \text{ Torr} \pm 0.1\%$, then removed the reactant and obtained a final reading of $0.10000 \text{ Torr} \pm 0.1\%$, as expected for this case of similar masses.

III. TOTAL RATE COEFFICIENTS

The inert gas ion signal, corrected for any minor changes in i_e , is measured at several reactant pressures to verify agreement with Eq. (2). (Data are shown in Ref. 10.) In all cases, the reactant concentration is less than 0.5% of the inert gas concentration, so that the diffusion coefficient of A⁺ in A is not influenced by the addition of reactant B. This procedure for determining the rate coefficient is repeated at many values of E/N by varying the electric field; the resulting rate coefficients are plotted as a function of the average center-of-mass collision energy in Figs. 2, 3, and 4.

A correction was necessary for the rate coefficients measured with Si₂H₆, since it was contaminated by sufficient silane to yield a fractional silane content of $37\% \pm 8\%$ of the total reactant density in the manifold and drift tube (determined by dissociative ionization mass spectrometer signals). Thus the apparent rate coefficient k_A measured with the contaminated gas is given by $k_A = k_2(1-f) + k_1f$, where k_1 and k_2 are the rate

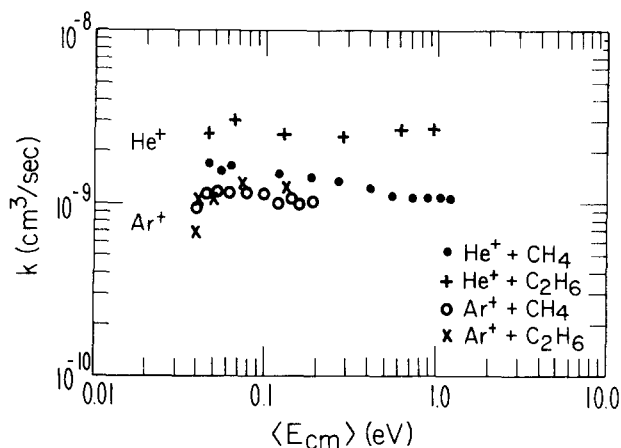


FIG. 2. Measured rate coefficients for He⁺ and Ar⁺ reactions with CH₄ and C₂H₆ as a function of mean center-of-mass collision energy.

coefficients for the inert gas reaction with silane and disilane, respectively, and $f=0.37$. The k_1 values are known from the silane measurements and are smaller than k_2 so that this correction is not a serious problem in the determination of k_2 .

The uncertainties in the measurement of the total rate coefficient are determined as follows. The drift velocities are reported⁷ to within 5% and checked in our apparatus for Ar⁺ in Ar to about this accuracy. The fluctuation in measurements of $\ln[A_0^+]/[A^+]$ is typically 7%. The uncertainty in the reactant gas density [B] is 9%, excluding the flow correction which adds an additional uncorrelated 10% for helium and 5% for neon. The total uncertainty in k , adding these in quadrature, is thus 13%–16%. For reactions with disilane, the additional uncertainty due to the silane contamination is 5%–10% which combines with the previous uncertainty to yield a 17% total uncertainty for all reactions with disilane. These uncertainties may be considered as one standard deviation.

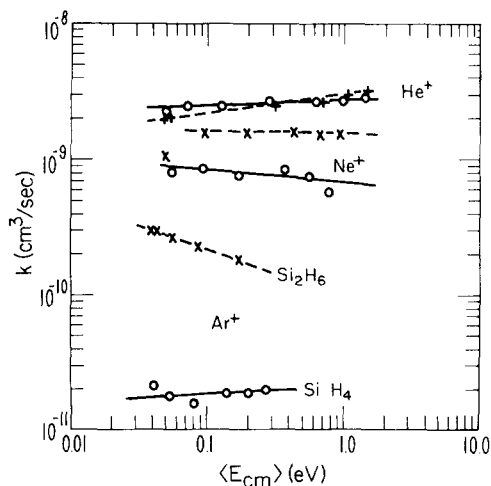


FIG. 3. Measured rate coefficients for He⁺, Ne⁺, and Ar⁺ reactions with SiH₄ and Si₂H₆ as a function of mean center-of-mass collision energy.

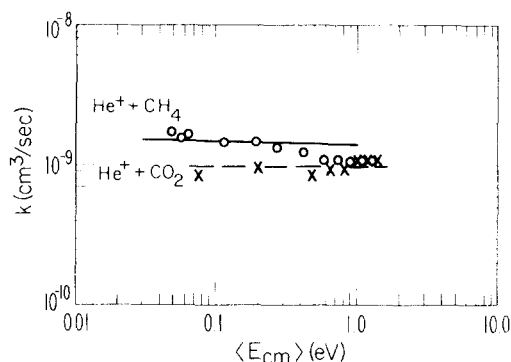


FIG. 4. Measured rate coefficients for He⁺ reactions with CH₄ and CO₂ as a function of mean center-of-mass collision energy. Points are present data, lines are averages through the data of Lindinger *et al* (Refs. 12 and 13).

In all cases but Ar⁺ + SiH₄, less than 0.1% reactant density was used, but in this case as much as 0.5% reactant density was necessary due to the small value of k . This amount of reactant could introduce three effects which would give erroneously large rate coefficients: (1) a reduction in the drift velocity of the inert gas ions, which increases the reaction time; (2) an increase in the transverse diffusion coefficient of the primary ions due to an increase in the ratio of the total energy to the energy in the field direction in a multi-component gas¹²; and (3) an increase in the silane flow through the 25 μ m orifice could occur due to somewhat viscous flow at $P_m=10$ Torr. The first two of these effects are negligible at the concentrations of SiH₄ used here. The third was taken into account by directly measuring the reactant pressure with the capacitance manometer to avoid this possible error. Thus we conclude that this large fractional SiH₄ concentration caused negligible additional uncertainty in k .

IV. PRODUCT IONS

The ionized products of these ion–molecule reactions have been measured with the mass spectrometer as a function of E/N . After taking into account the mass discrimination of the mass filter and the differential diffusive loss of product ions, as well as correcting for the isotopic contributions to the different silicon-containing ion signals, the product-ion signals are converted into percentages of the total ion signal for each E/N .

The sensitivity of the mass spectrometer and ion optics was determined by comparing, for each inert gas, the ion signals from the mass spectrometer to the total ion current collected on all the focusing lenses when the lenses were biased to collect all ions through the drift-tube orifice. The sensitivity is almost independent of M for $M=4$ and 20, but decreases by a factor of 2 at $M=40$ and a factor of 50 at $M=84$ (see Ref. 10). As the product-ion masses are between these inert gas masses, appreciable uncertainty arises due to interpolating the mass sensitivity curve, particularly for masses above 40.

The focusing voltages are set to maximize the prod-

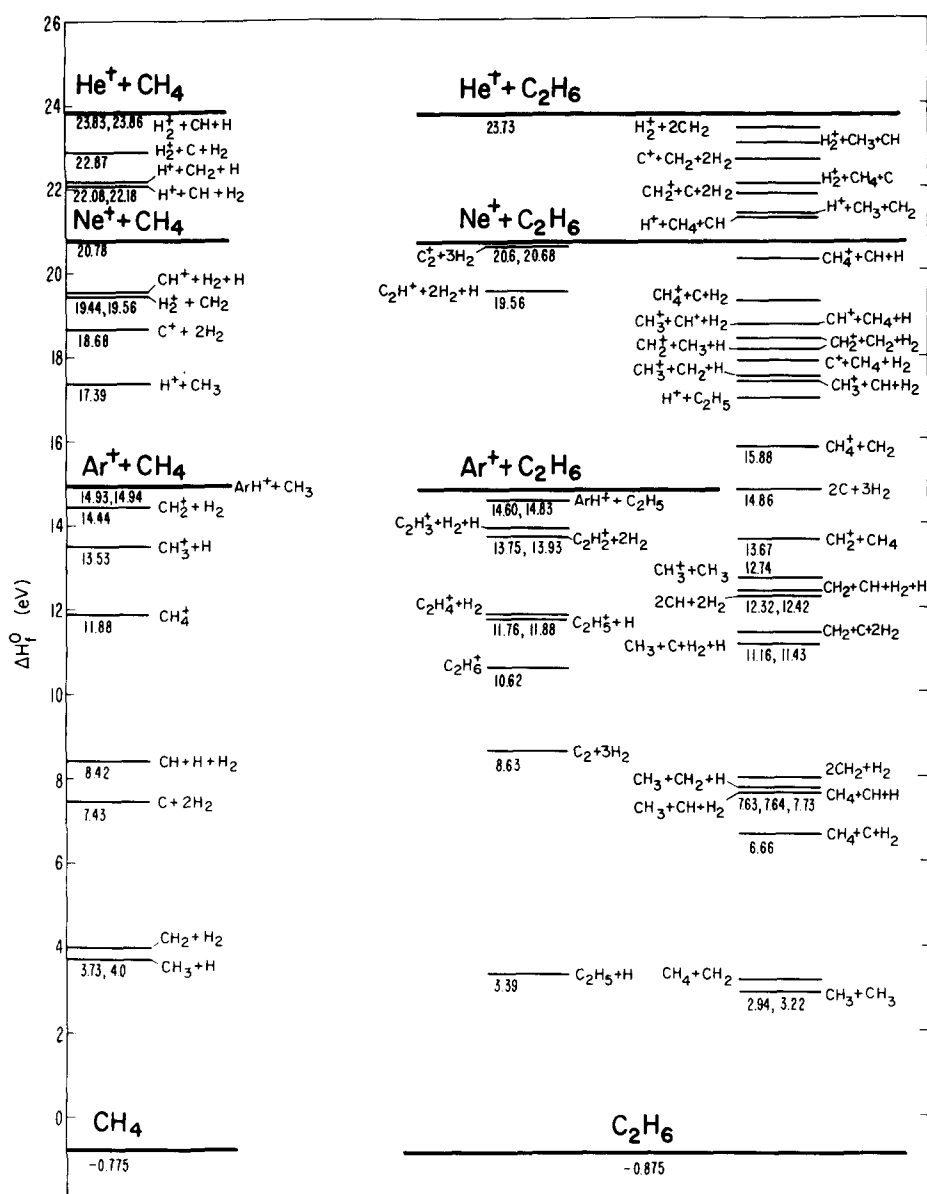


FIG. 5. Enthalpies for the reactions of the inert gas ions with CH₄ and C₂H₆, compiled from Refs. 13, 14, and 17.

uct-ion signals, with the constraint that the ratio of product-ion signals is not dependent on the settings. The focusing of the product ions is highly dependent on the ion kinetic energy, and considerable variation in product-ion ratios can occur due to their different energy distributions. From Wannier's expression, we expect the mean energy, and thereby the observed abundances of the heavier ions, to be relatively insensitive to the focusing voltages, whereas H⁺ will be most sensitive to focusing as it has the highest mobility and thereby the highest mean energy of all the product ions. This was, in fact, observed and the resultant uncertainty in H⁺ product fractions is roughly 30%.

A. Secondary ion diffusion—The H⁺ problem

Differential diffusive losses of product ions, before reaching the orifice at the end of the drift tube, occur because of different diffusion coefficients for the various product ions. Since products of similar mass are ex-

pected to have approximately the same diffusion coefficients, this requires a significant correction to the observed signals for H⁺ and minor (less than 10%) correction for CH_n⁺ vs C₂H_n⁺ or SiH_n⁺ vs Si₂H_n⁺. Ar⁺ does not have sufficient enthalpy to create significant H⁺ from any of the reactants (see Figs. 5 and 6 and Refs. 13–17), and for Ne⁺ we did not measure H⁺. Thus, only corrections for differential diffusion of H⁺ vs heavy reactants in He will be considered here. Details are given in Ref. 10, where a calculation is presented based on diffusion coefficients from Ref. 7 and drift-tube correction formulas from Ref. 18. Resulting corrections typically increase the H⁺ signals by a factor of 1.5 relative to all the heavier ions at $E/N=30$ Td. However, we have tested the correction by varying E/N from 30 to 70 Td at low E/N where the center-of-mass collision energy is slowly varying and the product distribution is expected to be constant. The correction shows a decrease of a factor of 2 to 3 in the H⁺ contribution relative to the heavier ions as E/N increases from 30 to 70 Td, pos-

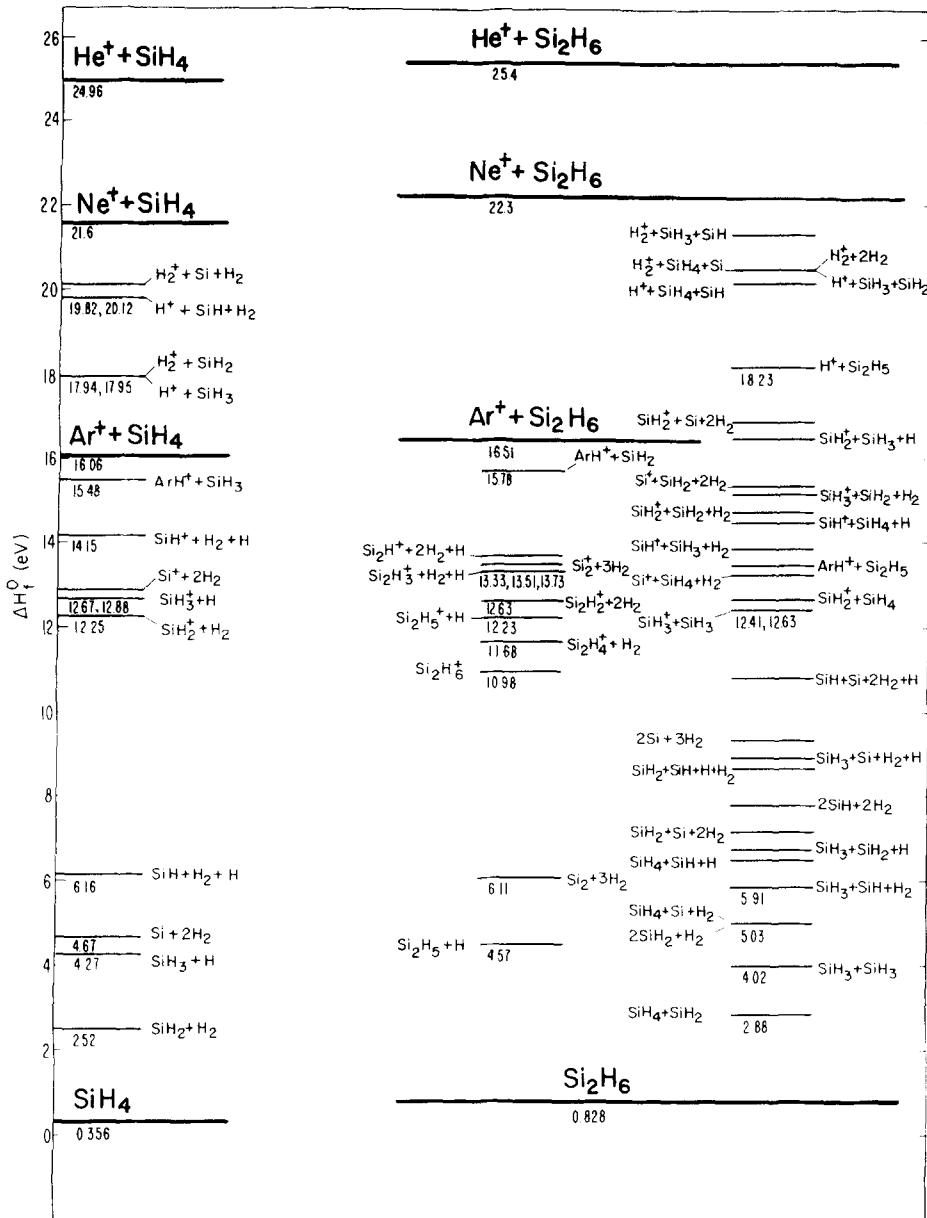


FIG. 6. Enthalpies for the reactions of the inert gas ions with SiH₄ and Si₂H₆, compiled from Refs. 13–16.

sibly due to changes in the mass spectrometer calibration efficiency for higher $\langle E_{\text{tr}} \rangle$. The diffusion-corrected H⁺ signals are 28%, 4%, 11%–28%, and 7% of the total product-ion signal for the reactions of He⁺ with SiH₄, Si₂H₆, respectively, at $E/N = 30$ Td. These are uncertain within perhaps a factor of 2. The H⁺ signal was not measured in neon so it is assumed, in assigning fractions to the other ions, that the H⁺ contribution for neon is the same as for helium (H⁺ is not a product of any reaction with Ar⁺; see Figs. 4 and 5). Product-ion ratios are plotted as rate coefficients by assuming a contribution from H⁺ of 25% at all E/N in CH₄ and SiH₄, and 10% at all E/N in C₂H₆ and Si₂H₆.

B. Secondary reactions

Reactions of the product ions with the neutral reactant B can change the product distribution unless $[B]k_s t \ll 1$, where k_s is the rate constant for secondary reactions and $t = L/2v_d^2$ is the average drift time for the

product ions. For most reactions, at a typical k_s of 10^{-9} cm³/s,¹ $[B]k_s t < 0.1$ at low E/N and less than 0.05 at high E/N (typically 30% of the initial inert gas ion signal was depleted for the reactant densities used). Thus fewer than 10% of the product ions are expected to have reacted at low E/N , as confirmed for several reactions by the lack of dependence of the product ions on the reactant density at low E/N . However, rate coefficients for the reactions of Ar⁺ with silane and disilane were so small that higher reactant densities (2×10^{13} and 3×10^{12} cm⁻³, respectively) were used and $[B]k_s t = 2$ and 0.3, respectively, resulted. (Product distributions could have been obtained at much lower reactant densities, but this was not done systematically.) Thus secondary reactions have a major effect on the product distributions measured at these relatively high reactant densities, as confirmed by the observation of disilane ions from Ar⁺ + SiH₄ reactions. One set of product ions for the Ar⁺ + SiH₄ product distribution was taken at $[B] = 3 \times 10^{12}$ cm⁻³ and at a center-

TABLE I. Ar⁺ + silane product distributions.

	From SiH ₄	From Si ₂ H ₆
Si ⁺	59%	5%
SiH ⁺	21%	8%
SiH ₂ ⁺	8.3%	
SiH ₃ ⁺	12%	
Si ₂ ⁺		18%
Si ₂ H ⁺		39%
Si ₂ H ₂ ⁺		14%
Si ₂ H ₃ ⁺		12%
Si ₂ H ₄ ⁺		
Si ₂ H ₅ ⁺		3%

of-mass collision energy of 0.1 eV ($E/N=280$ Td), for which we estimate that 25% of the product ions have probably undergone secondary reactions. In Table I, we give these data, plus those for Ar⁺ + Si₂H₆ at $\langle E_{cm} \rangle = 0.09$ eV, for which we estimate that 30% of the ions have undergone secondary reactions. The uncertainty in these data is large, but it is included as the only such data currently available.

At high values of E/N , the possibility of secondary, hydrogen-stripping reactions of the product ions with neutral inert gas atoms arises. Some of these reactions are endothermic by less than 2 eV, as determined from the heats of formation of the various ions listed in Figs. 5 and 6. Estimates of the E/N values at which the average center-of-mass collisional energy equals the enthalpy for these reactions reveal that a number are thermodynamically possible (see Ref. 10). However, the product-ion distributions observed are roughly independent of E/N whereas all of these reactions have thresholds above 0.3 eV (150 Td in He) and, in addition, the variations present in the product data can not be explained on the basis of such stripping reactions. Thus, this appears to have a negligible effect on the product distributions.

C. Doubly ionized ions

No He²⁺ and negligible Ne²⁺ are produced by 100 eV electrons, but Ar²⁺, present at 2% concentration, complicates reactions involving Ar⁺. At the reactant densities used, almost all of the Ar²⁺ reacts at all E/N , whereas roughly 50% of the Ar⁺ reacts at low E/N . Thus the fraction of secondary ions from Ar²⁺ vs those from Ar⁺ is 2/50 at low E/N and increases to 2/10 at high E/N . Indeed, the observation of the products C⁺ and CH⁺ at $\langle E_{cm} \rangle$ greater than 0.05 eV (E/N greater than 100 Td) in reaction of methane with argon are doubtless due to Ar²⁺, as these products are not energetically possible from Ar⁺ (see Fig. 5). Similarly, Ar²⁺ is probably the cause of the products C₂⁺ and C₂H⁺ observed in the reaction of argon with ethane above 0.1 eV (300 Td). It is unlikely that these products are produced by the hydrogen-stripping reactions discussed above.

D. Penning ionization by inert gas metastables

Penning ionization by He metastables can contribute to the very minor ion signals, as determined from the

following observations. When the repeller field is reversed (from +2 to -2 V), the CH_n⁺ product-ion signals and the He⁺ signal fall to less than 1% of their original levels, indicating that negligible Penning ionization is occurring outside the source. In addition, as the electron energy is decreased from 50 to 28 eV, the He⁺ and product-ion signals fall by roughly the same factor of 5 and the product-ion distribution is constant, indicating negligible Penning ionization in the source compared to primary (A⁺ + B) reactions in the drift tube. However, for the reaction He⁺ + CO₂, the He⁺, O⁺, and CO⁺ ion signals vanish when the repeller field is reversed (+2 to -2 V) but 25% of the CO₂⁺ signal remained (CO₂⁺ constituted 10% of the total product-ion signal, so that although only 10% of the He⁺ ion signal was converted into CO₂⁺, all of the helium metastables seem to have produced CO₂⁺). Helium metastables are known to react rapidly with CO₂,¹⁹ consistent with this observation. Thus, we conclude that if the other reactant gases act like CH₄ then the effect of He metastables is negligible. However, if the other reactant gases behave like CO₂, with all the metastables converting the reactant into one particular ion which is a small fraction of the ions produced by reactions with the inert gas ions, then the effect of metastables can be significant.

Finally, the ratio of the cross section for producing Ne metastables²⁰ to the Ne ionization cross section²¹ is smaller than the similar ratio for He, so that contributions to the product-ion signals from Ne metastables should be negligible (see Ref. 10). Ar metastable levels do not have enough energy to Penning ionize the reactants.

E. Other extraneous sources

Ar₂⁺, Ne₂⁺, and He₂⁺ have little effect on the product distributions because of their low concentrations (less than 0.1%).

The contribution to the product-ion signals from direct electron impact dissociative ionization of the reactant in the source can be estimated from the following. The contribution to a particular product-ion flux [C⁺] from A⁺ + B reactions is proportional to $i_e Q_A [A] k_C [B] t$, where Q_A is the electron impact ionization cross section for producing A⁺ from A and k_C is the ion-molecule reaction rate coefficient for producing C⁺. The contribution to this flux from direct ionization of the reactant in the source is proportional to $i_e Q_C [B]$, where Q_C is the electron collisional dissociative ionization cross section for producing C⁺ from B (e.g., SiH⁺ from SiH₄). Taking the ratio of these fluxes gives $Q_A [A] k_C t / Q_C$. All terms in this ratio are known, so that it can be calculated. As t decreases with increasing E/N , this ratio also decreases, so that the largest contributions to the product-ion signals from direct ionization occur at the highest values of E/N and are 3% for reactions with He⁺ and Ne⁺ and less than 1% for reactions of Ar⁺ with the alkanes. As can be inferred from the ratio, the largest contribution to a particular product-ion signal from direct ionization occurs for the product ion with the largest Q_C that simultaneously has a small k_C . Such a situation exists for SiH₂⁺ in helium, neon, and argon, with pre-

dicted contributions from the source of 25%, 10%, and 10% at low E/N and 45%, 20%, and 40% at high E/N , respectively.

F. Results

Results are shown in Figs. 7–10 and in Tables I and II.^{22–30} From the above considerations, we conclude that signals contributing more than 5% to the total product-ion signal have uncertainties of 10% and the smaller signals, of less than 5% of the total, have uncertainties of 100%. The H⁺ signals have uncertainties of 60%.

V. DISCUSSION

A comparison of our measurements of the total rate coefficients, versus $\langle E_{cm} \rangle$, for the reactions He⁺ + CH₄ and He⁺ + CO₂ shows good agreement with those of previous investigators^{22,31} (see Fig. 2). Table II gives a comparison of our rate coefficient measurements at low collision energies (~ 700 K) to other thermal measurements and to the Langevin rate coefficients. Our rate coefficient measurements at low collision energies agree within 15% with all but one of the previously measured thermal rate coefficients. The exception is the reaction Ar⁺ + SiH₄, discussed below.

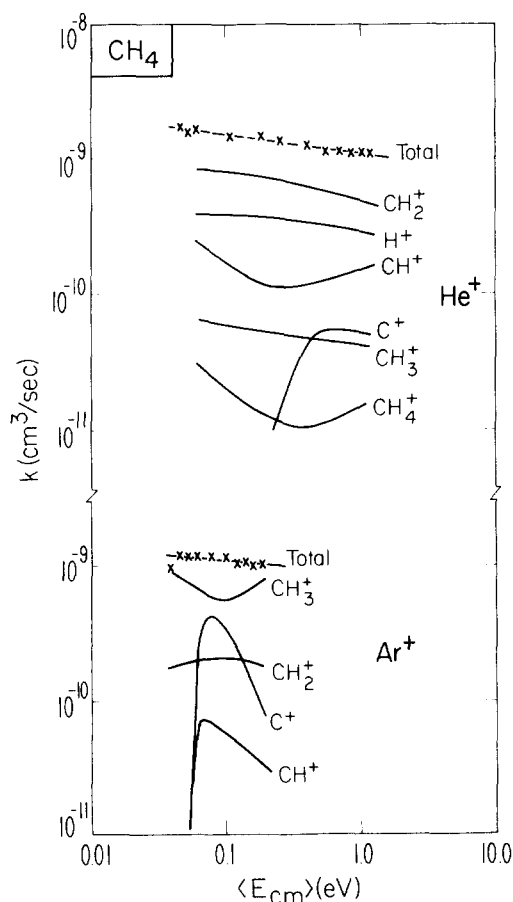


FIG. 7. Measured product-ion distributions for He⁺ and Ar⁺ reactions with CH₄ as a function of mean center-of-mass collision energy, plotted as rate coefficients. The H⁺ from He⁺ was measured only at $\langle E_{cm} \rangle < 0.1$ eV, and is extrapolated to higher energies as a constant fraction. The H⁺ ion was less than 0.1% from Ar⁺. H₂⁺ is less than 0.1% from both reactions.

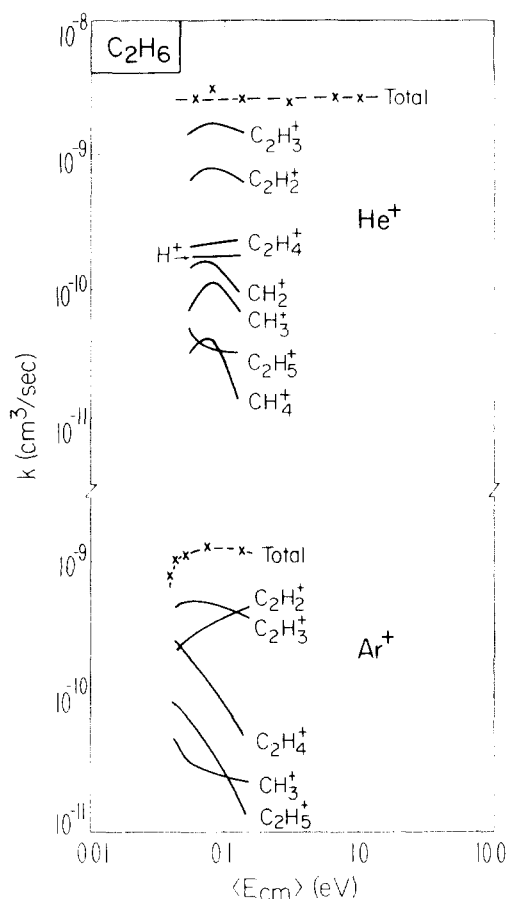


FIG. 8. Measured product-ion distributions for He⁺ and Ar⁺ reactions with C₂H₆ as a function of mean center-of-mass collision energy, plotted as rate coefficients. The H⁺ from He⁺ was measured only at $\langle E_{cm} \rangle < 0.1$ eV, and is extrapolated to higher energies as a constant fraction. The H⁺ ion was less than 0.1% from Ar⁺. H₂⁺ is less than 0.1% from both reactions.

The majority of the reactions measured here are fast, proceeding at near Langevin rates (Figs. 2–4 and Table II). The exception is the reactions of Ar⁺ with SiH₄ and Si₂H₆. Langevin (spiraling) rate coefficients are independent of collision energy, and since these coefficients

TABLE II. Ion-molecule rate coefficients.

Reaction	Present (700 K)	Rate coefficients ($\times 10^9$ cm ³ s ⁻¹)	
		Langevin	Previous (300 K)
He ⁺ + CO ₂	0.9	1.97	0.85 ^a , 1.2 ^b , 1.1 ^c , 1.0 ^d
He ⁺ + CH ₄	1.7	2.16	1.3 ^a , 1.6 ^c , 1.5 ^d , 1.3 ^e , 1.26 ^f , 1.25 ^g
Ar ⁺ + CH ₄	1.16	1.12	0.9 ^a , 1.34 ^c , 1.03 ^d , 0.98 ^h , 2.1 ⁱ , 1.9 ^j
He ⁺ + C ₂ H ₆	2.66	2.6	1.29 ^g
Ar ⁺ + C ₂ H ₆	1.15	1.22	1.07 ^g
He ⁺ + Si ₂ H ₄	2.4	2.58	2.18 ^g
Ne ⁺ + SiH ₄	0.85	1.39	0.85 ^g
Ar ⁺ + SiH ₄	0.017	1.16	0.10 ^g
He ⁺ + Si ₂ H ₆	1.71	3.3	
Ne ⁺ + Si ₂ H ₆	1.1	1.6	
Ar ⁺ + Si ₂ H ₆	0.3	1.3	

^aReference 23.

^bReference 24.

^cReference 4.

^dReference 22.

^eReference 25.

^fReference 26.

^gReference 27.

^hReference 28.

ⁱReference 29.

^jReference 30.

are large at the present experimental energies, additional (direct) charge-transfer processes are unlikely to have a large effect on the total reaction probability. This is indeed observed as the fast rate constants show little dependence on collision energy. Additionally, the center-of-mass collision energy ($\langle E_{cm} \rangle$) is nearly constant (thermal) at low E/N , whereas t_d , diffusion, and other experimental quantities are rapidly varying. Thus, at low E/N , the measured rate coefficients should be independent of E/N . This provides another test of the experimental accuracy, and it is indeed observed in all but one of the reactions measured here. The exception is the $\sim 40\%$ decrease in the rate coefficient for the reactions $\text{Ar}^+ + \text{C}_2\text{H}_6$ at the lowest $\langle E_{cm} \rangle$, which is believed to be some artifact of this particular measurement, but was not investigated further.

Rate coefficients that are much less than the Langevin values characteristically decrease with collision energy to a minimum and then increase again.^{8,32,33} An explanation for this behavior has been given by McFarland *et al.*⁸ and by Ferguson *et al.*³² They suggest that these slow reactions proceed by intermediate complex formation at low collision energies. As the lifetime of the complex decreases with increasing collision energy, they propose that the probability of reaction, proportional to this lifetime, will also decrease. The increase with collision energy, which generally occurs for $\langle E_{cm} \rangle > 0.1$ eV, is attributed to the breakdown of this model

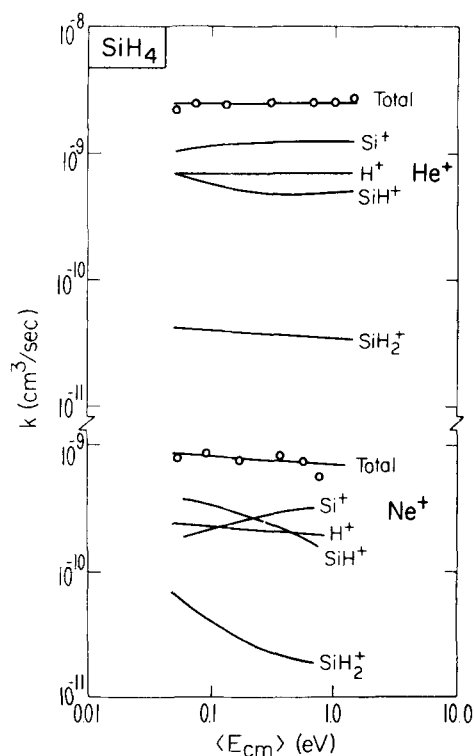


FIG. 9. Measured product-ion distributions for He⁺ and Ne⁺ reactions with SiH₄ as a function of mean center-of-mass collision energy, plotted as rate coefficients. The H⁺ from He⁺ was measured only at $\langle E_{cm} \rangle < 0.1$ eV, and is extrapolated to higher energies as a constant fraction. The H⁺ from Ne⁺ is assumed to be the same as for He⁺. H₂⁺ is less than 0.1% from both reactions.

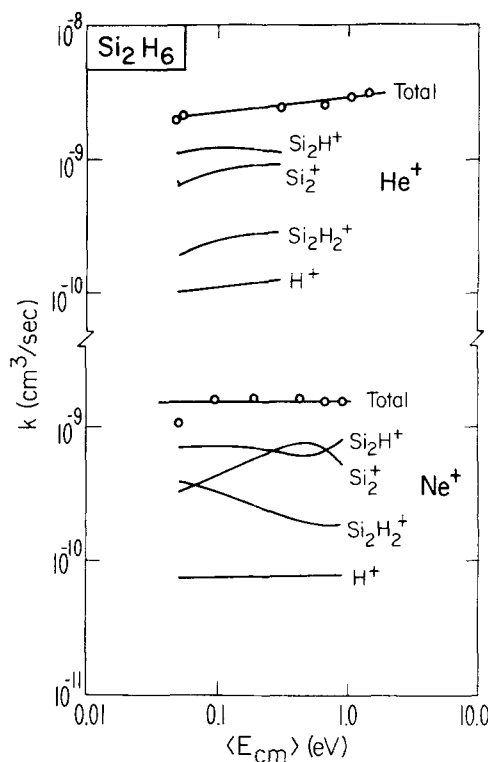


FIG. 10. Measured product-ion distributions for He⁺ and Ne⁺ reactions with Si₂H₆ as a function of mean center-of-mass collision energy, plotted as rate coefficients. The H⁺ from He⁺ was measured only at $\langle E_{cm} \rangle < 0.1$ eV, and is extrapolated to higher energies as a constant fraction. The H⁺ from Ne⁺ is assumed to be the same as for He⁺. H₂⁺ is less than 0.1% from both reactions.

and the onset of other processes. Such a decrease (below 0.1 eV) has been observed here in the slow reaction $\text{Ar}^+ + \text{Si}_2\text{H}_6$, for which $k \sim [\langle E_{cm} \rangle]^{-0.35}$ (Fig. 4). However, no such decrease is observed in the still slower $\text{Ar}^+ + \text{SiH}_4$ reaction. Many product-ion channels are exothermic for the reactions of Ar⁺ with SiH₄ and Si₂H₆ (Fig. 6) so it is not obvious why these two reactions are slow. It does not appear to be due to a long-range barrier, as this rate coefficient would then rise with $\langle E_{cm} \rangle$. It also appears possible, but unlikely, that it could be due to formation of a long-lived, metastable SiH_n⁺ ion that recovers its charge in a successive Ar collision via the reverse reaction. This type of "back reaction" has been observed in Ar⁺ + NO reactions.³⁴ However, just as was observed in that case, it appears highly likely that a major fraction of the successive Ar collisions with any such metastable ion will quench the ion to a stable state rather than transferring charge from the Ar. In addition, there are many exothermic SiH_n⁺ channels and we observe all of these product ions. Thus, it appears unlikely that transfer to one metastable state dominates the initial Ar⁺ reaction.

Many checks were made to be certain that the measurements of the Ar⁺ + SiH₄ rate coefficient were correct, such as the immediate comparison of this rate coefficient to the rate coefficient for the reaction Ar⁺ + CH₄, observation of the SiH_n⁺ product ions to definitely

TABLE III. He⁺ + CH₄ → products.

Product	Present	Adams and Smith ^b	Huntress <i>et al.</i> ^c
	754 K	300 K	300 K ^a
H ⁺	28%	25%	25%
CH ⁺	14%	26%	14%
CH ₂ ⁺	53%	53%	56%
CH ₃ ⁺	4%	5%	4%
CH ₄ ⁺	2%	1%	2%

^aA hydrogen-ion content of 25% has been assumed in the data of Ref. 26.

^bReference 35.

^cReference 26.

identify the reactant, the much larger amount of SiH₄ compared with the other reactants required to produce an observable decrease in the Ar⁺ signal, and other checks described above. Our measurement of this rate coefficient at low collision energies is a factor of 6 lower than the thermal rate coefficient measured in Ref. 25. As we have positive identification of the products of this reaction, we tend to believe our measurements.

A comparison, given in Table III, of our He⁺ + CH₄ product-ion data at $E/N = 35$ Td (corresponding to $T = 750$ K) with previously measured thermal distributions shows remarkable agreement. This further supports the conclusion that metastables and other ions have negligible effects on most of our product-ion distributions. The exception is the effect of Ar²⁺ on the reactions involving Ar⁺, as discussed above.

The fast reactions discussed below all proceed at near Langevin, or spiraling-complex (AB)⁺ formation rates, and they are independent of collision energy, as given by the Langevin model. Thus they appear to proceed via complex formation. The reactions of He⁺ with CH₄ is very exothermic. The large excess energy transferred to the CH₄⁺ electrons by the He⁺ + CH₄ → He + CH₄⁺ charge exchange within the (HeCH₄)⁺ complex must be dissipated to stabilize the products. Competition between stabilization by He removal leaving CH₄⁺, and by H removal leaving lighter CH_n⁺ ions, might favor the removal of H due to the lower mass and hence faster separation of the H. Combined with the large excess energy, this implies a tendency to remove many H atoms and/or an H⁺ to stabilize the remaining complex. This could explain the large fractions of H⁺ and of CH_n⁺ with $n < 3$ observed in the product distributions (Fig. 7). The same argument would predict little HeH⁺, as is observed. In the case of the reaction He⁺ + SiH₄, we observe even more highly stripped SiH_n⁺ as well as a larger fraction of H⁺ (Fig. 9). This is consistent with this model combined with the fact that the Si-H bond is weaker than the C-H bond. Applying the same argument to the reactions of He⁺ with C₂H₆ and Si₂H₆, we expect that the C-C and Si-Si bonds will rarely be broken compared with the C-H or Si-H bonds, because of the slower rate of dissociation of the C- or Si-containing fragments compared with the rate of H boiloff. Indeed, the product-ion data show that the C-C or Si-Si bond is rarely broken.

The product-ion distributions for the reactions of Ne⁺

with SiH₄ and Si₂H₆ are very similar to those for He⁺, indicating that the same arguments may apply to the Ne⁺ reactions. These reactions have somewhat less excess energy, but the Ne is heavier and slower than the He. In the case of the reactions of Ar⁺ with the alkanes (C_nH_{2n+2}), there is only 1–4 eV of excess energy, with the largest excess for the product ions C_nH_{2n+2}⁺ ($n = 1, 2$). These two ions must stabilize by Ar boiloff, however, whereas the lighter C_nH_m⁺ result from the faster H boiloff. Thus, the same argument again predicts more highly stripped ions within the exothermic channels (the H⁺ product-ion channel is not exothermic for all reactions with Ar⁺ studied here). This again is what is observed.

The case of the reactions of Ar⁺ with the silanes, which have much smaller rate coefficients, shows the same general pattern in the product distribution. This may be due to the same competition between boil-off rates, but as these rate coefficients are so small this could be quite a different process.

One might compare the product-ion distributions from these charge-exchange reactions to the distributions resulting from electron-collisional dissociative ionization or photoionization of CH₄, C₂H₆, SiH₄, and Si₂H₆, for electron or photon energies equal to the enthalpies of the various ion-molecule reactions (see Figs. 5 and 6). However, we believe that this is unlikely to give any additional information regarding these reactions for the following reasons: The charge-exchange process, within the AB⁺ complex, produces a highly excited B⁺ ionic state which must stabilize by dissociation or separation from A. The electron-collision produces a distribution of excited *neutral* molecular states, some of which stabilize by ionization. In contrast to the ion-collision process, the electron(s) can carry off the majority of the excess energy. The photoabsorption also produces a highly excited *neutral* molecule, which again can stabilize to an ion by electron removal of much of the excess energy. Thus it is not surprising that ions from electron impact and photoionization tend to be more hydrogen rich (see Ref. 10).

This work was supported in part by Solar Energy Research Institute contract XB-2-02085-1. The authors are grateful to Dr. Veronica Bierbaum and Dr. A. V. Phelps for helpful discussions.

¹T.-Y. Yu, T. M. H. Cheng, V. Kempter, and F. W. Lampe, *J. Phys. Chem.* **79**, 3321 (1972).

²E. E. Ferguson, F. C. Fehsenfeld, and A. L. Schmeltekopf, *Adv. At. Mol. Phys.* **5**, 1 (1969).

³T. B. McMahon and J. L. Beauchamp, *Rev. Sci. Instrum.* **43**, 509 (1972); W. T. Huntress, Jr. and R. F. Pinzzotto, *J. Chem. Phys.* **59**, 4742 (1973).

⁴N. G. Adams and D. Smith, *Int. J. Mass Spectrom. Ion Phys.* **21**, 349 (1976).

⁵E. W. McDaniel, D. W. Martin, and W. S. Barnes, *Rev. Sci. Instrum.* **33**, 2 (1962); J. Heimerl, R. Johnson, and M. A. Biondi, *J. Chem. Phys.* **51**, 5041 (1969).

⁶E. W. McDaniel, V. Cermak, A. Dalgarno, E. E. Ferguson, and L. Friedman, *Ion-Molecule Reaction* (Wiley-Intersci-

- ence, New York, 1970).
- ⁷H. W. Ellis, R. Y. Pai, E. W. McDaniel, E. A. Mason, and L. A. Viehland, *At. Data Nucl. Data Tables* **17**, 177 (1976).
- ⁸M. McFarland, D. L. Albritton, F. C. Fehsenfeld, E. E. Ferguson, and A. L. Schmeltekopf, *J. Chem. Phys.* **59**, 6620 (1973).
- ⁹G. H. Wannier, *Bell Syst. Tech. J.* **32**, 170 (1953); *Phys. Rev.* **83**, 281 (1951).
- ¹⁰H. Chatham, Thesis, University of Colorado, 1983.
- ¹¹E. W. McDaniel, *Collision Phenomena in Ionized Gases* (Wiley, New York, 1964).
- ¹²H. S. Hahn and E. A. Mason, *Phys. Rev. A* **7**, 1407 (1973).
- ¹³*JANAF Thermochemical Tables*, 2nd ed., NSRDS-NBS-37 (U.S. GPO, Washington, D.C., 1971).
- ¹⁴*JANAF Thermochemical Tables*, 1978 Supplement, *J. Phys. Chem. Ref. Data* **7**, 793 (1978).
- ¹⁵R. Walsh, *Acc. Chem. Res.* **14**, 246 (1981).
- ¹⁶P. Potzinger and F. W. Lampe, *J. Phys. Chem.* **73**, 3912 (1969).
- ¹⁷J. L. Franklin, J. G. Dillard, H. M. Rosenstock, J. T. Hemon, K. Draxl, and F. H. Field, *Natl. Stand. Ref. Data Ser. Natl. Bur. Stand.* **26**, (1969).
- ¹⁸Y. Kaneko, L. R. Megill, and J. B. Hasted, *J. Chem. Phys.* **45**, 3741 (1966).
- ¹⁹A. L. Schmeltekopf and F. C. Fehsenfeld, *J. Chem. Phys.* **53**, 3173 (1970).
- ²⁰F. A. Sharpton, R. M. St. John, C. C. Lin, and F. E. Fajen, *Phys. Rev. A* **2**, 1305 (1970).
- ²¹D. A. Rapp, P. Englander-Golden, and D. D. Briglia, *J. Chem. Phys.* **42**, 4081 (1965).
- ²²W. Lindinger, E. Alge, H. Stori, R. N. Varney, H. Helm, P. Holzmann, and M. Pahl, *Int. J. Mass Spectrom. Ion Phys.* **30**, 251 (1979).
- ²³R. C. Bolden, R. S. Hemsworth, M. J. Shaw, and N. T. Twiddy, *J. Phys. B* **3**, 45 (1970).
- ²⁴F. C. Fehsenfeld, A. L. Schmeltekopf, P. D. Goldan, H. C. Schiff, and E. E. Ferguson, *J. Chem. Phys.* **44**, 4087 (1966).
- ²⁵M. T. Bowers and D. D. Elleman, *Chem. Phys. Lett.* **16**, 486 (1972).
- ²⁶W. T. Huntress, Jr., J. B. Laudenslager, and R. F. Pinizzotto, Jr., *Int. J. Mass Spectrom. Ion Phys.* **13**, 331 (1974).
- ²⁷J. B. Laudenslager, W. T. Huntress, Jr., and M. T. Bowers, *J. Chem. Phys.* **61**, 4600 (1974).
- ²⁸P. Ausloos, J. R. Eyler, and S. G. Lias, *Chem. Phys. Lett.* **30**, 21 (1975).
- ²⁹C. E. Melton, *J. Chem. Phys.* **33**, 647 (1960).
- ³⁰J. Gaughhofer and L. Kevan, *Chem. Phys. Lett.* **16**, 492 (1972).
- ³¹W. Lindinger, D. L. Albritton, and F. C. Fehsenfeld, *J. Chem. Phys.* **62**, 4957 (1975).
- ³²E. E. Ferguson, D. K. Bohme, F. C. Fehsenfeld, and D. B. Dunkin, *J. Chem. Phys.* **50**, 5039 (1969).
- ³³I. Dotan and W. Lindinger, *J. Chem. Phys.* **76**, 4972 (1982).
- ³⁴I. Dotan, F. C. Fehsenfeld, and D. L. Albritton, *J. Chem. Phys.* **71**, 3289 (1979).
- ³⁵N. G. Adams and N. Smith, *J. Phys. B* **9**, 1439 (1976).